Four-Way Spoof Surface Plasmon Polaritons Splitter/Combiner

Shi-Yan Zhou, Sai-Wai Wong, *Senior Member, IEEE*, Jing-Yu Lin, *Student Member, IEEE*, Lei Zhu, *Fellow, IEEE*, Yejun He, *Senior Member, IEEE*, and Zhi-Hong Tu, *Member, IEEE*

***Abstract*— Corrugated metal with period grooves supports spoof surface plasmons polariton (SSPP) wave in microwave and terahertz ranges. In this letter, a four-way SSPP splitter/combiner with oval-ring periodic structures is presented by using a single connection junction. Up to the authors' best knowledge, a four-way SSPP splitter/combiner is never reported in the literature. In order to verify the performance of the mentioned SSPP splitter/combiner, we have manufactured and tested the presented SSPP splitter/combiner. The simulation and measurement results demonstrate that the designed conversion between a single coplanar waveguide junction and four SSPP waveguides is high efficiency. The SSPP splitter equally separates the electromagnetic wave into four paths. Hence, the proposed four-way splitter is expected to develop the SSPP active and passive components and relative integrated circuits.**

***Index Terms*— Coplanar waveguide (CPW), four-way splitter/combiner, spoof surface plasmon polariton (SSPP).**

I. Introduction

SURFACE plasmon polariton (SPP) is the confined wave that propagates along the interface between substrate and metal in optical frequency. The SPP wave has the ability to confine electromagnetic (EM) fields to subwavelength dimensions, enabling the fabrication of miniaturized photonic devices and highly integrated optical circuits [1]. However, the metal with uniform perfect electric conductor property does not support the SPP at low frequencies. In order to take advantage of the unique property of SPP in the microwave and terahertz bands, the conductors with periodic holes or grooves are used to propagate spoof surface plasmon polariton (SSPP) mode [2], [3]. Recently, there are many types of SSPP transmission lines reported [4], [5]. These designed SSPPs-based devices have the virtues of the controllable ultra-wide operating frequency bandwidth [6], low transmission loss [7], and low crosstalk loss [8].

The multiple way splitter/combiner [9]–[11] plays an important role in the microwave components and integrated circuits, which can be used in array antennas, phase shifter, power amplifiers, and so on. The SSPP devices have attracted great interest in recent years. The radio frequency front-end components of SSPP antennas [12], [13] and SSPP amplifier [14] have been investigated. In addition, two two-way SSPP power dividers [15], [16] have been designed. Those SSPP power dividers consist of one composite SSPP waveguide and two symmetrical branches. However, those reported methods are not convenient to separate the SSPP transmission line into more channels.

In this letter, we present an SSPP splitter to realize the four equal divisions of SPP EM waves in a single printed circuit board metal layer. In previous studies, the proposed two-way power divider [16] split one oval-ring SSPP waveguide into two half oval-ring branches. To increase the transmission paths, we design the conversion section with four half oval-ring SSPP waveguides by using single coplanar waveguide (CPW) connection junction. The simulation and measurement show that the proposed four-way splitter equally divides an EM wave into four ways in the operating frequency band. The proposed four-way SSPP splitter/combiner has the potential to further facilitate the study of the SSPP components and systems in microwave and terahertz frequency bands.

II. Dispersion Graph

As is shown in Fig. 1, the dispersion curves of the SSPP transmission lines and the light line are calculated by the eigenmode solver of the commercial software CST. The SSPP transmission line consists of cascaded half oval-ring-shaped cells, whose material is copper with the thickness of 0.017 mm. The thickness of the underlying substrate is 0.8 mm, and the relative permittivity is 2.55 (1 + i0.0029). At the low frequency, the wave vectors k_x of the light line and the SSPP transmission lines are very close to each other. As the frequency increasing, the curves of the SSPP transmission lines gradually move away from the curve of the light line. This implies that the wavelength of the SSPP transmission line is shorter than the wavelength of the light line. Due to this

Manuscript received September 28, 2018; revised November 15, 2018; accepted December 5, 2018. Date of publication January 4, 2019; date of current version February 14, 2019. This work was supported in part by the Shenzhen Science and Technology Programs under grant JCYJ 20180207154824493, in part by the Natural Science Foundation of Guangdong Province under Grant 2018A030313481, in part by Shenzhen University Research Startup Project of New Staff under Grant 20188082, in part by the NTUT-SZU Joint Research Program under Grant 2018009, and in part by the Fundamental Research Funds for the Central Universities under Grant 2017ZD044 and Grant 2017ZD055. *(Corresponding author: Sai-Wai Wong.)*

S.-Y. Zhou, J.-Y. Lin, and Z.-H. Tu are with the School of Electronic and Information Engineering, South China University of Technology, Guangzhou 510640, China.

S.-W. Wong and Y. He are with the College of Information Engineering, Shenzhen University, Shenzhen 518060, China (e-mail: wongsaiwai@ieee.org).

L. Zhu is with the Department of Electrical and Computer Engineering, University of Macau, Macau 999078, China.

Color versions of one or more of the figures in this paper are available online at http://ieeexplore.ieee.org.

Digital Object Identifier 10.1109/LMWC.2018.2886318

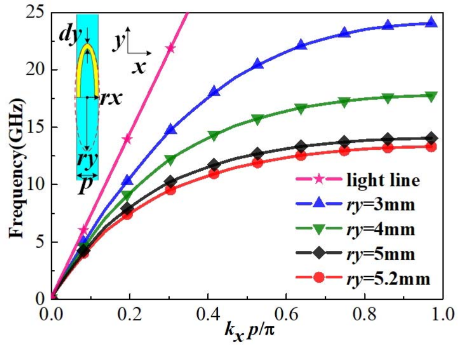

Fig. 1. Dispersion graph of light line and designed SSPP transmission lines with a long axis radius of different lengths. Periodic SSPP cells are constructed by half oval rings, in which $rx = 1.2$, $dy = 0.5$, and $p = 2.1$ (all in mm).

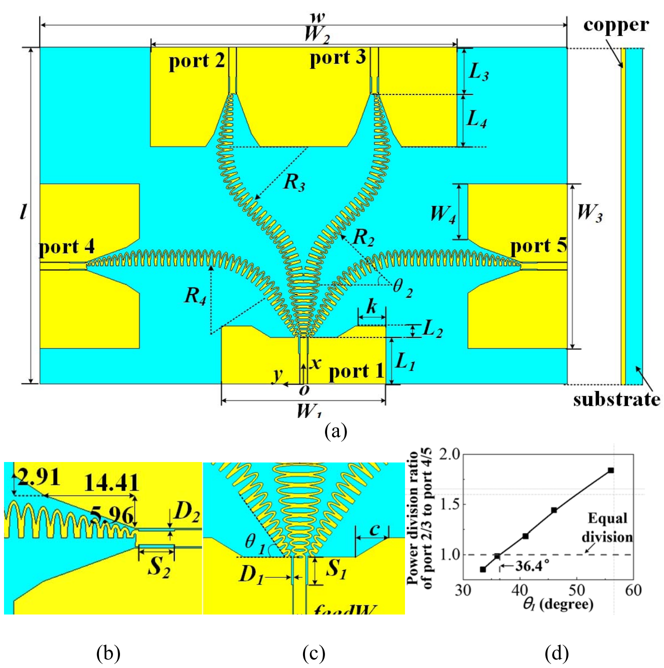

Fig. 2. Configuration of a four-way SSPPs splitter/combiner. (a) Front view (left) and cross-sectional view (right) of the four-way splitter, $l = 168.6$, $w = 107.7$, $W_1 = 52.7$, $W_2 = 98.0$, $W_3 = 52.7$, $W_4 = 17.65$, $k = 9.65$, $L_1 = 15$, $L_2 = 3.66$, $L_3 = 15$, $L_4 = 16.78$, $\theta_2 = 45°$, $R_2 = 28$, $R_3 = 24$, and $R_4 = 24$. (b) Dimensions of the conversion section connected to port 5, $S_2 = 5.0$ and $D_2 = 0.4$. (c) Dimensions of the conversion section connected to port 1, feed $W = 2.3$, $c = 6.0$, $S_1 = 5.0$, $D_1 = 0.4$, and $\theta_1 = 36°$. (d) Relationship between the angle θ_1 and the power division ratio of port 2/3 to port 4/5 (all in mm).

feature, SSPP devices make a contribution to the development of miniaturization and high integration. Moreover, as the long axis radius of the ellipse increases, the cutoff frequency of the SSPP transmission lines gradually drops to a lower frequency. Wherein, the cutoff frequency of the SSPP transmission line is 12.5 GHz when the long axis radius is 5.2 mm.

III. Four-Way SSPP Splitter/Combiner

Fig. 2 gives the schematic of the designed four-way SSPP splitter/combiner. The SSPP waveguides with half oval-ring cells are connected to a 50-Ω CPW transmission line. The proposed four-way splitter/combiner consists of four similar SSPP waveguides with the periodic array of half oval rings,

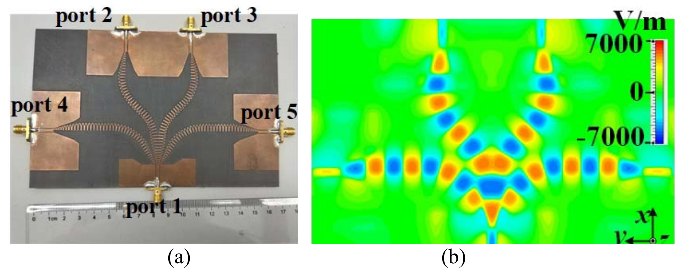

Fig. 3. (a) Photography of the designed four-way SSPPs splitter/combiner. (b) Simulated near-field distributions at 7.5 GHz.

which is described in Fig. 2(a). The whole structure is symmetric along the center vertical axis.

Fig. 2(b) marks the dimensions of four identical transition sections at four output ports. Fig. 2(c) marks the dimensions of the 1-to-4 transition section at input port. The transition section is required to match the wave vector and the impedance between the CPW mode and the SSPP mode. As illustrated in Fig. 1, the cutoff frequency gradually decreases when the long axis radius of the ellipses increases. Thus, several oval-ring cells with gradient long axis radius are adopted to match the wave vector. In order to match the impedance, the stepped impedance is added between the CPW and the SSPP waveguides. And then, compare with the design of two-way splitter in [16], the flaring ground parts are replaced by two SSPP waveguides with gradient long axis radius. The CPW can be thought of as two slot lines, feeding EM energy to four SSPP waveguides. Meanwhile, the SSPP transmission line with double gratings fed by a slotline is reported in [17]. The power division ratio is controlled by the angle θ_1 as shown in Fig. 2(d). When the angle θ_1 is equal to 36.4°, an equal power division is obtained. Meanwhile, when the θ_1 increases, the power division ratio of port 2/3 to port4/5 increases.

IV. Experimental Results

In order to verify the properties of the designed four-way SSPP splitter/combiner, we have fabricated and tested the circuit. As shown in Fig. 3(a), the five ports of the proposed four-way splitter are connected to 50-Ω SubMiniature version A connectors. The simulated near-field distribution of the proposed splitter is shown in Fig. 3(b). The simulated electric field of E_z component is 2 mm above the copper layer. It is obvious that the fed EM energy is divided into four-branch equal division. The S-parameters of the SSPP splitter are measured by the Agilent N5230A vector network analyzer. We first tested the transmission coefficient $|S_{21}|$. The port 1 and port 2 are connected to the vector network analyzer. Meanwhile, the rest ports (port 3, port 4, and port 5) are connected to three 50-Ω matching loads, respectively. According to the same method, the $|S_{31}|$, $|S_{41}|$, and $|S_{51}|$ are subsequently obtained.

Fig. 4 demonstrates the simulation and measurement results of the proposed splitter/combiner. The simulation results are calculated by the time-domain solver of the CST software. In Fig. 4(a), the measured results show that the 10-dB bandwidth of the transmission coefficient is approximately 7.745 GHz from 2.105 to 9.85 GHz. The minimum measured

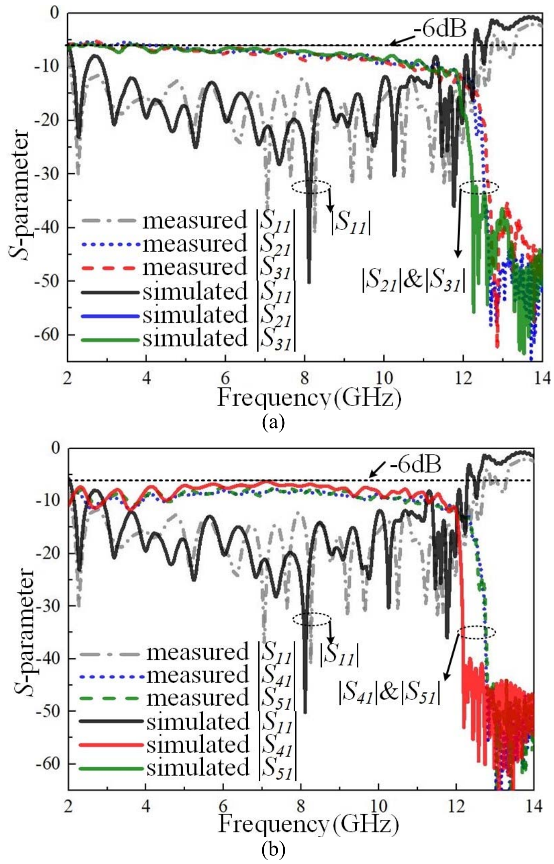

Fig. 4. Simulated and measured S-parameters of the proposed four-way SSPP splitter/combiner, in which the simulated results are the solid lines and the measured results are the dashed lines. (a) $|S_{11}|$, $|S_{21}|$, and $|S_{31}|$. (b) $|S_{11}|$, $|S_{41}|$, and $|S_{51}|$.

TABLE I
COMPARISON WITH THE TRADITIONAL SPLITTERS

Ref	RL (dB)	FBW	IL (dB)	N	TL Technology	Application in flexible materials
[1]	19	8	6 ± 1.1	2	Microstrip	No
[2]	12	50	6.48	2	Microstrip	No
[3]	10	93	6.8 ± 0.4	2	Microstrip and Slotline	No
This work	11.9	129	7.8	1	SSPP	Yes

Ref: Reference; RL: Return Loss; FBW: Fractional Bandwidth; IL: Insertion Loss; N: Number of copper layers; TL: Transmission Line.

insertion loss is 7.8 dB. Moreover, the $|S_{11}|$ is lower than 11.95 dB in the measured bandwidth. However, the difference of the experiment and simulation of the $|S_{41}|$ and $|S_{51}|$ is about 1 dB. The difference between the simulated and measured results is attributed to the tolerance and metal roughness in fabrication processing. The proposed splitter is successful to equally divide the SPP wave into four ways in the operating band.

A comparison of the traditional four-way splitter with the designed SSPP splitter is shown in Table I. Compared to the traditional devices, the SSPPs-based four-way splitter has the advantage with ultra-wide bandwidth, single copper layer, and application in flexible materials.

V. CONCLUSION

In this letter, a four-way SSPPs splitter/combiner of half oval-ring units has been proposed. The long axis of the half oval ring has the impact on the cutoff frequency, which is used to design the transition section to match the wave vector between the CPW and the SSPP waveguide. And then, the transition section between the CPW and four SSPP waveguides is designed to split the EM wave into four paths with equal magnitude. The inclination angle between the two SSPP transmission lines with gradient long axis radius affects the power division ratio. In addition, the measurement and simulation of the designed four-way SSPP splitter indicate a reasonable agreement. The presented four-way SSPP splitter has the potential application in microwave advanced integrated circuits and wireless communication systems.

REFERENCES

[1] W. L. Barnes, A. Dereux, and T. W. Ebbesen, "Surface plasmon subwavelength optics," *Nature*, vol. 424, pp. 824–830, Aug. 2003.

[2] X. Shen, T. J. Cui, D. F. Martin-Cano, and J. Garcia-Vidal, "Conformal surface plasmons propagating on ultrathin and flexible films," *Proc. Nat. Acad. Sci. USA*, vol. 110, no. 1, pp. 40–45, Jan. 2013.

[3] H. F. Ma, X. Shen, Q. Cheng, W. X. Jiang, and T. J. Cui, "Broadband and high-efficiency conversion from guided waves to spoof surface plasmon polaritons," *Laser Photon. Rev.*, vol. 8, no. 1, pp. 146–151, 2014.

[4] A. Kianinejad, Z. N. Chen, and C.-W. Qiu, "Full modeling, loss reduction, and mutual coupling control of spoof surface plasmon-based meander slow wave transmission lines," *IEEE Trans. Microw. Theory Techn.*, vol. 66, no. 8, pp. 3764–3772, Aug. 2018.

[5] A. Kianinejad, Z. N. Chen, and C.-W. Qiu, "Low-loss spoof surface plasmon slow-wave transmission lines with compact transition and high isolation," *IEEE Trans. Microw. Theory Techn.*, vol. 64, no. 10, pp. 3078–3086, Oct. 2016.

[6] X.-L. Tang, Q. Zhang, S. Hu, A. Kandwal, T. Guo, and Y. Chen, "Capacitor-loaded spoof surface plasmon for flexible dispersion control and high-selectivity filtering," *IEEE Microw. Wireless Compon. Lett.*, vol. 27, no. 9, pp. 806–808, Sep. 2017.

[7] H. C. Zhang, Q. Zhang, J. F. Liu, W. Tang, Y. Fan, and T. J. Cui, "Smaller-loss planar SPP transmission line than conventional microstrip in microwave frequencies," *Sci. Rep.*, vol. 6, Mar. 2016, Art. no. 23396.

[8] H. C. Zhang, T. J. Cui, Q. Zhang, Y. Fan, and X. Fu, "Breaking the challenge of signal integrity using time-domain spoof surface plasmon polaritons," *ACS Photon.*, vol. 2, no. 9, pp. 1333–1340, Aug. 2015.

[9] F.-J. Chen, L.-S. Wu, L.-F. Qiu, and J.-F. Mao, "A four-way microstrip filtering power divider with frequency-dependent couplings," *IEEE Trans. Microw. Theory Techn.*, vol. 63, no. 10, pp. 3494–3504, Oct. 2015.

[10] K. Song, Y. Mo, and Y. Fan, "Wideband four-way filtering-response power divider with improved output isolation based on coupled lines," *IEEE Microw. Wireless Compon. Lett.*, vol. 24, no. 10, pp. 674–676, Oct. 2014.

[11] K. Song, Y. Mo, Q. Xue, and Y. Fan, "Wideband four-way out-of-phase slotline power dividers," *IEEE Trans. Ind. Electron.*, vol. 61, no. 7, pp. 3598–3606, Jul. 2014.

[12] J. Y. Yin *et al.*, "Frequency-controlled broad-angle beam scanning of patch array fed by spoof surface plasmon polaritons," *IEEE Trans. Antennas Propag.*, vol. 64, no. 12, pp. 5181–5189, Dec. 2016.

[13] A. Kianinejad, Z. N. Chen, L. Zhang, W. Liu, and C.-W. Qiu, "Spoof plasmon-based slow-wave excitation of dielectric resonator antennas," *IEEE Trans. Antennas Propag.*, vol. 64, no. 6, pp. 2094–2099, Jun. 2016.

[14] H. C. Zhang, S. Liu, X. Shen, L. H. Chen, L. Li, and T. J. Cui, "Broadband amplification of spoof surface plasmon polaritons at microwave frequencies," *Laser Photon. Rev.*, vol. 9, no. 1, pp. 83–90, Nov. 2014.

[15] X. Gao *et al.*, "Ultra-wideband surface plasmonic Y-splitter," *Opt. Express*, vol. 23, no. 18, pp. 23270–23277, 2015.

[16] S. Zhou *et al.*, "Spoof surface plasmon polaritons power divider with large isolation," *Sci. Rep.*, vol. 8, no. 5947, Apr. 2018, Art. no. 5947.

[17] X. Gao, L. Zhou, Z. Liao, H. F. Ma, and T. J. Cui, "An ultra-wideband surface plasmonic filter in microwave frequency," *Appl. Phys. Lett.*, vol. 104, no. 19, p. 191603, 2014.